Synthesis, transport and hypoxia-selective binding of 1-β-D-(5-deoxy-5-fluororibofuranosyl)-2-nitroimid-azole (β-5-FAZR), a configurational isomer of the clinical hypoxia marker, FAZA

Saeed Emami [1,*], Piyush Kumar [2], Jennifer Yang [2], Zbigniew Kresolic [2†], Robert Paproski [3,4], Carol Cass [3,4], Alexander JB McEwan [2,4], Leonard I Wiebe [1,2,3]

[1] Faculty of Pharmacy and Pharmaceutical Sciences, and [4]Department of Oncology, University of Alberta, Edmonton, Alberta, Canada T6G 2N8, and Departments of [2] Oncologic Imaging and [3]Experimental Oncology, Cross Cancer Institute, 11560 University Avenue, Edmonton, Alberta, Canada T6G 1Z2

[*] **Current address:** Department of Medicinal Chemistry, Faculty of Pharmacy, Mazandaran University of Medical Sciences, Sari, Iran.

† deceased

Dedicated to the memory of our colleague and friend Prof. A.A. Noujaim.

Received 31 October 2006; Revision received 15 November; Accepted 23 November 2006, Published June 14th 2007

Abbreviations: PET, positron emission tomography; SPECT, single-photon emission computed tomography; OER, oxygen enhancement ratio; FMISO, fluoro-misonidazole; [^{18}F]FAZA, 1-α-D-(5-deoxy-5-[^{18}F]fluoro-arabinofuranosyl)-2-nitroimidazole; β-5-FAZR, 1-β-D-(5-fluoro-5-deoxyribofuranosyl)-2-nitroimidazole; β-AZR, 1-β-D-(ribofuranosyl)-2-nitro-imidazole; α-AZR, α-azomycin riboside; TBDPS-Cl, tert.-butylchlorodiphenylsilane; TBDPS-AZR, 1-β-D-(5-O-tert.-butyldiphenylsilylribo-furanosyl)-2-nitroimidazole; DAST, diethylaminosulfur-trifluoride; hNTs, human nucleoside transporters; hENT, human equilibrative nucleoside transporter; hCNT, human concentrative nucleoside transporter; HCT116/100 human colorectal carcinoma cell line; IC_{50}, concentration that inhibited transport activity by 50%; PBS, phosphate buffer saline; EDTA, ethylene-diaminetetraacetic acid; $CDCl_3$, deuterated chloroform; CD_3OD, deuterated methanol; TMS+, tetramethylsilane; PMR-NOE, proton magnetic resonance spectroscopy Nuclear Overhauser Effect.

Keywords: β-5-FAZR, [^{18}F]FAZA, hypoxia, PET tracer, nucleoside transport, radiosensitization.

ABSTRACT – Purpose: Cellular uptake of most azomycin-based radiosensitizers depends on perfusion and diffusion, rather than on active transport. In medical imaging using radioisotopically-labeled azomycin nucleosides, image contrast depends on rapid diffusion from normoxic tissues and rapid renal clearance from the central compartment. [^{18}F]FAZA [1-α-D-(5-deoxy-5-[^{18}F]fluoroarabinofuranosyl)-2-nitroimidazole], an azomycin nucleoside currently under clinical evaluation as a marker of tissue hypoxia in medical centers world-wide, provides high contrast but its uptake is diffusion dependent and therefore low. 1-β-D-(5-Fluoro-5-deoxyribofuranosyl)-2-nitro-imidazole **6** (β-5-FAZR), a β-ribose analog of FAZA, has now been developed to exploit transport across cell membranes to improve absolute uptake in hypoxic regions and high contrast. **Methods:** β-5-FAZR was synthesized by classical sugar-base coupling followed by regioselective fluorination. *In vitro* radiosensitization of hypoxic and normoxic cells to ^{60}Co x-rays was determined relative to known radiosensitizers. The relative abilities of the human equilibrative nucleoside transporters (hENT1 & hENT2) and the human concentrative nucleoside transporters, hCNT1, hCNT2 and hCNT3, to bind the radiosensitizers were determined by quantifying their inhibition of [^{3}H]uridine transport by recombinant transporters produced in yeast. **Results:** β-5-FAZR was synthesized in 44 percent yield. β-5-FAZR had moderate radiosensitization effect on human HCT116/100 colorectal carcinoma (OER 1.8). β-5-FAZR was a weak inhibitor of uridine transport relative to non-fluorinated 1-β-D-(ribofuranosyl)-2-nitroimidazole (β-AZR). **Conclusion:** Facile synthesis of β-5-FAZR was achieved and its activity as a radiosensitizer was confirmed. Substitution of C'-5 hydroxyl by fluorine in the ribose moiety greatly reduced interaction with hENT1/2 and hCNT1/2 and moderately reduced interaction with hCNT3 relative to thymidine and β-AZR.

Corresponding author: Dr. Piyush Kumar, Department of Oncologic Imaging, Cross Cancer Institute, 11560 University Avenue, Edmonton, Alberta, Canada T6G 1Z2; E-mail: piyushku@cancerboard.ab.ca; Phone: +1.780.989.4313; Fax: +1.780.432.8483

INTRODUCTION

Imaging techniques such as positron emission tomography (PET), single-photon emission computed tomography (SPECT) and magnetic resonance imaging (MRI) can provide *in vivo* visualization of biological processes and metabolic pathways at cellular and molecular levels (1)
Selective uptake of radiotracers in various pathological disorders, including benign tumors cancers, can be used to identify molecular targets, monitor therapeutic efficacy, and develop new treatment modalities. Hypoxia, a confounding characteristic of many clinical disorders, results from transient capillary occlusion, poorly organized vascular architecture (2,3), irregular blood flow (4-7) or arterial damage, or inadequate angiogenesis. The negative effects of hypoxia in radiation therapy of cancer are the subject of many reports (8,9). In human tumors it is a prognostic feature that is associated with an aggressive clinical and biological phenotype (1). The hypoxic microenvironment within tumors promotes both local invasion and distant metastasis (1,8) and is associated with resistance to anticancer therapies, in particular, ionizing radiation (10).

For radiolabeled nitroimidazoles, adduct formation in the virtual absence of O_2 (hypoxia) is the basis for selective radiotracer accumulation and imaging in target tissues. Specificity of adduct formation in only those cells that are hypoxic is attributable to the oxygen-reversible one-electron reduction of the nitro substituent. In the absence of oxygen, reductive formation of chemically-reactive species by metabolically-viable reductases leads to adduct formation with a range of cellular components. Such adduct formation, especially with macromolecules, not only prevents egress of the nitroimidazole but importantly, results in the oxygen mimicking effect of trapping radiation-induced molecular defects that cause radiosensitization. The electron reduction potential (11) and water-lipid partition (12) are critical properties that affect their selectivity for hypoxic cells and influence their efficacy and toxicity.

1-α-D-(5-Deoxy-5-[^{18}F]fluoroarabinofuranosyl)-2-nitroimidazole (13,14) ([^{18}F]FAZA), a PET radiotracer that selectively accumulates in hypoxic cells, is currently used in cancer patients in several medical centres to assess tumor hypoxia (15,16). FAZA has the α-configuration around C-1' (Figure 1) and is not a natural permeant for nucleoside transporters. The hypoxia-specific uptake of FAZA is therefore attributable only to organ perfusion, its diffusion through cell membranes, and its rapid clearance from non-hypoxic (i.e. non-target) regions of the body. Although FAZA uptake is quantitatively similar to other clinical hypoxia PET tracers such as fluoromisonidazole (FMISO), it provides superior image contrast (17,18). *In vivo* PET imaging with [^{18}F]FAZA has shown correlation between hypoxia levels and treatment response to gefitinib in A431 xenografts, thereby demonstrating the potential value of assessing hypoxia as part of a therapeutic protocol (19).

Membrane transport of physiological nucleosides and many nucleoside analogs is mediated by nucleoside transporters (reviewed in 20). Human nucleoside transporters (hNTs) belong to two structurally unrelated protein families: the equilibrative nucleoside transporters (hENTs, four isoforms) and the concentrative nucleoside transporters (hCNTs, three isoforms). hENT1 and hENT2 mediate non-concentrative bidirectional transport of nucleosides across membranes and hENT3 and hENT4 are pH dependent. hCNT1, hCNT2 and hCNT3 are symporters that use the electrochemical gradient of sodium to drive inward transport of nucleosides into cells. hENT1/2 exhibit broad permeant selectivities, are widely distributed in the body and are found in many tumor types. hENT3 is a broadly selective organellar transporter found in many tissue types. hENT4 is highly selective for adenosine and appears to be limited primarily to cardiac tissue. hCNT1/2 accept primarily pyrimidine and purine nucleosides, respectively, as permeants and hCNT3 exhibits broad permeant selectivity. hCNTs are found primarily in specialized epithelia, including kidney and gastrointestinal tract, and hCNT3 appears to be more widely distributed than hCNT1/2 (21). The distribution of CNTs in tumor tissues has not been widely explored. The present work describes an effort to develop a fluorinated nitroimidazole radiodiagnostic tracer which has structural similarities to FAZA, so that reduction potential and lipophilicity are not affected substantially, but with a beta nucleoside configuration to facilitate its transport into hypoxic cells by the five major hNTs of plasma membranes (hENT1/2, hCNT1/2/3).

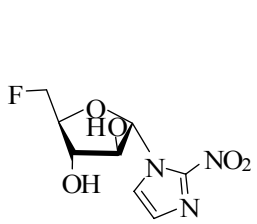

FAZA

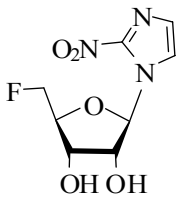

β-5-FAZR

Figure 1. Structures of FAZA and β-5-FAZR

The synthesis, *in vitro* radiosensitization and capacity to interact with hNTs of 1-β-D-(5-deoxy-5-fluororibofuranosyl)-2-nitroimidazole (β-5-FAZR), a molecule designed to meet these requirements, are now reported.

MATERIALS AND METHODS

Chemistry

All chemicals used were reagent grade. β-AZR was prepared using a literature procedure. Solvents were dried over appropriate drying agents and freshly distilled before use. The progress of synthetic reactions was monitored by thin layer chromatography (TLC) using 250 μm Whatman MK6F silica gel micro TLC plates and $CHCl_3$:MeOH (95:5, v/v, solvent system A; 90:10, v/v, solvent system B) as developing solvent. Column chromatography was performed on Merck silica gel 60 (particle size 70-200 and 230-400 mesh ASTM). Melting points were determined on a Büchi capillary melting point apparatus and are uncorrected. ^1H and ^{13}C NMR spectra were recorded on a Bruker AM-300 spectrometer in deuterated chloroform ($CDCl_3$) or methanol (CD_3OD), depending on the solubility of the product. Chemical shifts are reported in ppm downfield with respect to tetramethylsilane as an internal standard. The protons and carbons of the sugar moiety and nitroimidazole are represented by a single prime (') and no prime, respectively. When necessary, high resolution mass spectra (HRMS) were recorded using an AEI-MS-12 mass spectrometer.

1-β-D-(5-O-tert.-butyldiphenylsilyl-2,3-di-O-acetyl-ribofuranosyl)-2-nitroimidazole ***(3).*** Tert.-butyl-diphenylsilyl chloride (TBDPS-Cl; 0.26 mL, 1.15 mmol) was added drop wise to a solution of azomycin riboside **2** (β-AZR; 270 mg, 1.1 mmol) in anhydrous pyridine (2 mL) at 22 °C and the mixture was allowed to stir under an inert atmosphere for 16 h. TLC examination (solvent system A) of the reaction mixture at this time showed no sign of **2**. The resulting 5'-O-silylated derivative TBDPS-AZR was acetylated *in situ* with acetic anhydride (0.42 mL, 4.0 mmol) under stirring for 16 h. Excess acetic anhydride was then hydrolyzed by adding ice to the reaction vessel, followed by removal of the solvent *in vacuo* on a rotary evaporator. Purification of the residue on a silica gel column, using ethyl acetate/toluene (30:70, v/v) as eluent, yielded 0.48 g (77 %) of pure **3**. M.P.:,52-53°C; ^1H NMR ($CDCl_3$+1% TMS), δ ppm: 1.12 (s, 9H, tert- butyl), 2.06 and 2.15 (two s, 6H, each for 3H of CH_3), 3.79 (dd, $J_{4',5'}$ = 2.13, Jgem = 12.2 Hz, 1H, H-5'), 4.14 (dd, $J_{4',5''}$ = 1.83, Jgem = 12.2 Hz, 1H, H-5"), 4.30 (ddd, $J_{3',4'}$ = 6.1 Hz, $J_{5',4'}$ = 1.96 Hz, $J_{5'',4'}$ = 2.13 Hz, 1H, H-4'), 5.58 (dd, $J_{2',3'}$ = 5.2 Hz, $J_{1',2'}$ = 3.1 Hz, 1H, H-2'), 5.61 (dd, $J_{2',3'}$ = 5.2 Hz, $J_{4',3'}$ = 6.1 Hz, 1H, H-2'), 6.63 (d, $J_{2',1'}$ = 3.1 Hz, 1H, H-1'), 7.01 (s, 1H, imidazole H-4), 7.39-7.49 (m, 6H of two phenyls), 7.64-7.68 (m, 4H of two phenyls) and 7.86 (s, 1H imidazole H-5); ^{13}C NMR ($CDCl_3$), δ ppm: 19.30 (tert. C), 20.36 and 20.47 (two CH_3 of $COCH_3$), 27.02 (CH_3 of TBDPS group), 61.93 (C-5'), 68.44 (C-4'), 75.41 (C-3'), 82.50 (C-2'), 89.61 (C-1'), 122.3 (imidazole C-4), 127.97 (C-4 of two phenyls), 128.67 (imidazole C-5), 130.08 and 130.20 (C-3 and C-5 of two phenyls), 131.86 and 132.5 (C-1 of two phenyls), 135.40 and 135.65 (C-2 and C-6 of two phenyls), 168.90 and 169.25 (two C=O) ppm; HRMS: for $C_{28}H_{33}N_3O_8NaSi$ Calc. 590.19291, Found 590.19269 (M^+Na 100%).

1-β-D-(2',3'-di-O-acetylribofuranosyl)-2-nitro-imidazole ***(4).*** Potassium fluoride (325 mg, 5.6 mmol) and benzoic acid (683 mg, 5.6 mmol) were

added to a solution of **3** in acetonitrile (20 mL) and the mixture was heated at 75-80 °C for 16 h. TLC (solvent system A) at this time indicated absence of the starting material **3**. The mixture was cooled to room temperature (22 °C) and filtered. The filtrate was evaporated to dryness and the viscous impure mass was subjected to column chromatography. Elution with ethyl acetate/hexanes (70:30, v/v) afforded pure **4** (248 mg, 93%). M.P.: 122-123°C; ^{1}H NMR ($CDCl_3$+1% TMS), δ ppm: 2.11 and 2.16 (two s, 6H, each for 3H of CH_3), 3.86 (dd, $J_{4',5'}$ = 1.96, Jgem = 12.5 Hz, 1H, H-5'), 4.09 (dd, $J_{4',5"}$ = 2.14, Jgem = 12.5 Hz, 1H, H-5"), 4.30 (ddd, $J_{3',4'}$ = 6.4 Hz, $J_{5',4'}$ = 1.96 Hz, $J_{5",4'}$ = 2.14 Hz, 1H, H-4'), 5.46 (dd, $J_{4',3'}$ = 6.4 Hz, $J_{2',3'}$ = 5.5 Hz, 1H, H-3'), 5.56 (dd, $J_{3',2'}$ = 5.5 Hz, $J_{1',2'}$ = 3.05 Hz, 1H, H-2'), 6.61 (d, $J_{2',1'}$ = 3.05 Hz, 1H, H-1'), 7.17 (s, 1H, imidazole H-4), 8.02 (s, 1H, imidazole H-5); ^{13}C NMR ($CDCl_3$), δ ppm: 20.36 and 20.51 (two CH_3), 60.61 (C-5'), 68.93 (C-4'), 75.68 (C-3'), 82.78 (C-2'), 89.71 (C-1'), 122.3 (imidazole C-4), 127.97 (imidazole C-5), 168.96 and 170.04 (two C=O) ppm; HRMS: for $C_{12}H_{15}N_3O_8Na$ Calc. 352.07514, Found 352.07553 (M^+Na 100%).

1-β-D-(5-fluoro-5-deoxyribofuranosyl)-2-nitro-imidazole ***(β-5-FAZR, 6).*** A solution of **4** (228 mg, 0.69 mmol) in anhydrous dichloromethane (25 mL) was cooled to -20 °C, and then treated with diethylaminosulfurtrifluoride (DAST; 335 mg, 0.27 mmol). Once the addition of DAST was complete, the temperature was slowly raised to 0-5 °C over 24 h. Catalytic amounts of anhydrous pyridine (0.25 mL) were used to facilitate nucleophilic fluorination. The reaction to form 1-β-D-(5-fluoro-5-deoxy-2,3-di-O-acetylribofuranosyl)-2-nitro-imidazole **5** was considered complete once **4** was no longer detectable by TLC (solvent system B). Excess DAST was decomposed by addition of NH_3/methanol (2 mL; 2 M) with stirring for 5 min. The solvent was removed from the reaction mixture under vacuum and an additional volume of NH_3/MeOH solution (15 mL; 2 M) was added to the crude residue to initiate deacetylation. The reaction mixture was stirred for 16 h at 22 °C, then evaporated to dryness. The resulting viscous material containing **6** was subjected to silica gel column chromatographic purification, using CH_2Cl_2:MeOH (96:4; v/v) as eluent, to afford 1-β-D-(5-deoxy-5-fluororibofuranosyl)-2-nitroimidazole, **6** (75 mg, 44%)**.** M.P.: 150-153 °C; ^{1}H NMR (CD_3OD), δ ppm: 4.03 (dd, $J_{5',4'}$ = 1.9 Hz, $J_{5",4'}$ = 1.8 Hz, $J_{F\text{-}4'}$ = 12.5 Hz, 1H, H-4'), 4.06 (dd, $J_{4',3'}$ = 6.4 Hz, $J_{2',3'}$ = 5.5 Hz, 1H, H-3'), 4.12 (dd, $J_{3',2'}$ = 5.5 Hz, $J_{1',2'}$ = 3.05 Hz, 1H, H-2'), 4.49 (ddd, $J_{4',5'}$ = 1.9 Hz, Jgem = 11.0 Hz, $J_{F\text{-}5'}$ = 45.8 Hz Hz, 1H, H-5'), 4.80 (ddd, $J_{4',5"}$ = 1.8 Hz, Jgem= 11.0 Hz, $J_{F\text{-}5"}$ = 48.8.0 Hz, 1H, H-5"), 6.25 (d, $J_{2',1'}$ = 3.05 Hz, 1H, H-1'), 7.02 (s, 1H, imidazole H-4), 7.57 (s, 1H imidazole, H-5,); ^{19}F NMR (CD_3OD), δ ppm: 104.13 (ddd, $J_{H5'\text{-}F}$ = 45.8 Hz, $J_{H5"\text{-}F}$ = 48.8 Hz, $J_{H4'\text{-}F}$ = 12.6 Hz); ^{13}C NMR (CD_3OD), δ ppm: 69.08 (d, $J_{F\text{-}C}$ = 8.7 Hz, C-3'), 77.64 (C-2'), 82.48 (d, $J_{F\text{-}C}$ = 170.29 Hz, C-5'), 83.85 (d, $J_{F\text{-}C}$ = 25.4 Hz, C-4'), 94.37 (C-1'), 123.5 (imidazole C-4), 128.7 (imidazole C-5) ppm; HRMS: for $C_8H_{10}N_3O_5FNa$ Calc. 270.04967, Found 270.04939 (M^+Na 100%).

Radiosensitization

Cell radiosensitization was determined using a ^{60}Co x-ray source together with a clonogenic survival assay (22). Briefly, HCT116/100 colorectal carcinoma cells (300,000 cells in 3 mL DMEM/F12 medium per T60 petri dish) were incubated under 5% CO_2 in air at 37 °C for 20 h. The dishes were assigned to either the control (normoxic) or hypoxic groups , the test substance (stock solution 10 mM in 95 % ethanol) was added to these groups to achieve a concentration of 100 μM and the incubatation was allowed for 30 min. Those in the hypoxic group were de-gassed to hypoxia by 6 consecutive vacuum and nitrogen fill cycles in a vacuum chamber. The Petri dishes (hypoxic and normoxic controls) were incubated for 30 min on an oscillating shaker at R/T X 60 cycles per min and then irradiated in a ^{60}Co γ-irradiator at 0 (control), 4, 8, 12, 16 and 20 Gy in N_2 (hypoxic sub-group) and air chambers (normoxic sub-group). The cells were then recovered from each dish by two consecutive washes with PBS followed by the addition of trypsin (500 μL) and quenching with fresh medium (4.5 mL). Cells were then plated at densities from 100 to 15000 cells/5 mL medium for normoxic conditions and 100 & 5000 cells/5 mL medium for hypoxic conditions. The cells were incubated for 10 to 14 days at 37 °C under 5% CO_2, then stained with methylene blue or crystal violet in ethanol, clones counted and surviving fractions were calculated. Data for β-5-FAZR and FAZA, both at 100 μM in HCT116 cells are presented in Figure 2. Tests were done in triplicate.

Transport

The binding of test compounds to hENT1/2 and hCNT1/2/3 was measured by monitoring the abilities of test compounds to inhibit [^{3}H]uridine transport in yeast cells producing recombinant hNTs (See ref 23-25 for construction of yeast strains and procedures for "inhibitor-sensitivity" assay). Briefly, yeast cells producing recombinant hENT1, hENT2, hCNT1, hCNT2, or hCNT3 were maintained in complete minimal medium (CMM) containing 0.67% yeast nitrogen base (Difco, Detroit, MI), and 2% glucose (CMM/Glu) to an OD_{600} of 0.8–1.5. Yeast cells were washed three times with fresh CMM/GLU (pH 7.4) and resuspended to an OD_{600} of 4 in CMM/GLU (pH 7.4). [^{3}H]Uridine (2 μM; Moravek Biochemicals, Brea, CA) and test compounds at desired concentrations in CMM/GLU (pH 7.4) were preloaded into 96-well plates. Transport was initiated by adding an equal volume of yeast suspension at OD_{600}=4 to individual wells of preloaded 96-well plates and terminated 10 min later by harvesting (Micro96 Harvester; Molecular Devices, Ca) the yeast cells of each plate onto binding enhanced filtermats (Molecular Devices, Ca) with continuous washing by distilled, de-ionized water to remove unincorporated permeant. The filter discs with yeast cells for each transport assay were placed into individual scintillation counting vials to which scintillation counting fluid (5 mL; EcoLite™, MP Biomedicals, Irvine, CA) was added. Scintillation vials were allowed to sit at room temperature overnight with shaking before counting. The amount of [^{3}H]uridine associated with yeast in the presence of 10 mM uridine was determined as nonspecifically associated radioactivity and was subtracted from total radioactivity for each transport assay. Data were fitted to theoretical inhibition curves by nonlinear regression to obtain IC_{50} values (concentration that inhibited [^{3}H]uridine transport by 50%). All experiments were carried out in quadruplicate.

RESULTS

Chemistry

Previous approaches to the synthesis of 1-β-D-(ribofuranosyl)-2-nitroimidazole (β-AZR), the precursor for β-5-FAZR, were based on the Lewis acid [e.g., $Hg(CN)_2$] catalyzed coupling of 2-nitroimidazole with 1-(O-methyl)-2,3,5-tri-O-acetylribofuranose, after bromination at C-1 with 40-48% hydrogen bromide (HBr) in glacial acetic (26). This conventional coupling procedure affords β-AZR in unsatisfactory yield due to the formation of α-AZR, a side product, and other decomposition products during the course of the reaction. Following an improved coupling procedure (27), 1-β-D-(2,3,5-tri-O-benzoylribofuranosyl)-2-nitroimidazole was obtained in >71% yield; which followed debenzoylation (2M NH_3/MeOH) to afford β-AZR, **2**, the main synthon for chemistry development of β-5-FAZR. Site-specific fluorination of **2** at the C-5 (ribofuranosyl) position (identified as C-5' in NMR assignments) was a pre-requisite for the development of β-5-FAZR, **6**; this requires a freely available hydroxyl group at the 5'-position while the remaining -OH groups at positions 2'- and 3'- remain unavailable for fluorination. This was achieved by silylating **2** with TBDPS-Cl in anhydrous pyridine at 22 °C for 16 h to give a putative intermediate 5'-O-silyl ether, 1-β-D-(5-O-tert.-butyldiphenylsilylribofuranosyl)-2-nitroimidazole (TBDPS-AZR), which was not isolated. This silyl ether, upon acetylation with acetic anhydride *in situ,* afforded 1-β-D-(5-O-tert.-butyldiphenylsilyl-2,3-di-O-acetylribofuranosyl)-2-nitroimidazole **3** in 77% yield. Selective desilylation at the 5'- position of **3** was facilitated by potassium fluoride and benzoic acid to afford 1-β-D-(2,3-di-O-acetylribofuranosyl)-2-nitro-imidazole **4** (93%). Nucleophilic fluorination at 5'-OH was achieved by treating **4** with DAST in anhydrous dichloromethane at -20 °C and then slowly raising the temperature to 0-5°C over 24 h. It was observed that fluorination yield is substantially reduced due to the formation of secondary products if the temperature is not controlled around 0 °C. Catalytic amounts of anhydrous pyridine were also required to facilitate nucleophilic fluorination. *In situ* decomposition of excess DAST and deacetylation were facilitated by the addition of 2M NH_3/MeOH solution to the crude residue which, ultimately, afforded the target molecule 1-β-D-(5-deoxy-5-fluororibofuranosyl)-2-nitroimidazole, **6** in 44% yield (Scheme 1).

Incorporation of fluorine in a molecule has significant impact on the chemical shifts and spin-spin coupling constants of the atoms where it is substituted, and upon the neighboring protons and groups (28).

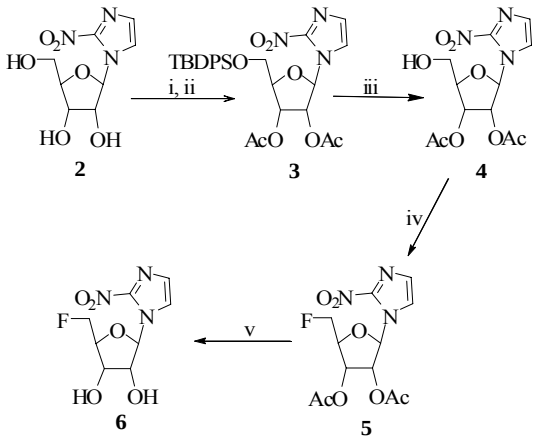

Scheme 1. Synthesis of β-5-FAZR. Reaction conditions: i) TBDPS/anhy. pyridine/22 °C; ii) acetic anhydride/pyridine/22 °C; iii) potassium fluoride/benzoic acid acid/70 °C; iv) DAST/CH_2Cl_2/0-5 °C; v) 2M NH_3/methanol. Bz = Benzoyl; Ac = Acetyl; TBDPS = Tert.-butylchlorodiphenylsilane.

Appearance of a *ddd* ($J_{H5'-F}$ = 45.8 Hz, $J_{H5''-F}$ = 48.8 Hz and $J_{H4'-F}$ = 12.6 Hz) in the ^{19}F NMR spectrum of β-5-FAZR confirmed the incorporation of fluorine at C-5' of **6**. Additional selective *F-H* and *F-C* spin-spin interactions between the atoms at 5'-, 4'- and 3'- positions ($J_{F-C5'}$ = 170.3 Hz (*d*); $J_{F-H4'}$ = 12.5 Hz and $J_{F-C4'}$ = 25.4 Hz (*d*); $J_{F-H3'}$ = 2.44 Hz (*d*) and $J_{F-C3'}$ = 8.7 Hz (*d*)) of the molecule confirmed the substitution of fluorine atom at 5'-position and the formation of β-5-FAZR, **6**.

Radiosensitization

Moderate *in vitro* radiosensitization of HCT116 colorectal carcinoma by β-5-FAZR was observed, with a calculated oxygen enhancement ratio (OER) of 1.8. Radiosensitization data for FAZA (left panel) and β-5-FAZR (right panel) in HCT116 cells are presented in Figure 2.

Uridine Transport

Interaction of hENT1/2 and hCNT1/2/3 with β-5-FAZR, β-AZR, and, for comparison, thymidine was evaluated by determining their relative sensitivities to inhibition of uptake of [^{3}H]uridine using an assay described elsewhere (23,25). IC_{50} values, which provide a measure of relative affinities of the transporters for test compounds, are given in Table 1. Compared to thymidine, β-5-FAZR showed moderate inhibition of [^{3}H]uridine transport by hCNT3 (IC_{50} values, respectively for β-5-FAZR and thymidine = 65±4 and 35±5 μM). IC_{50} values for β-5-FAZR were >500 μM for the other hNTs tested (rank order: hCNT1< hENT2 < hENT1 << hCNT2).

DISCUSSION

The synthesis of β-5-FAZR proceeded as anticipated using classical nucleoside chemistry approaches (29, 30). Insertion of fluorine at ribose

C-5' was demonstrated unequivocally by both F-19 and proton NMR. Radiosensitization was similar to that for FAZA in HCT116 cells (OER ~ 1.8) and to that previously reported for β-5-IAZR in EMT-6 cells (31), also at 100 μM. Data presented here and from other studies (29, 30, 32) indicates that C-5' substitution and C-1' configuration of the sugar moiety has little impact on the reduction/adduct formation properties of the nitroimidazole moiety, as expected from PMR-NOE and x-ray crystallographic studies in the 5-iodosugar nucleosides (33). Transport of AZR by the equilibrative erythrocyte transporter known today as hENT1 has also been reported previously (34) but not by other members of the hENT family or by members of the hCNT family.

Table 1. Inhibition of [^{3}H]uridine transport by β-5-FAZR, AZR and thymidine in yeast expressing recombinant hNTs.

Nucleoside Transporter	Comparative inhibitory concentrations (IC_{50}; μM)		
	Thymidine	β-AZR	β-5-FAZR
hENT1	76 ± 18	170 ± 22	1600 ± 140
hENT2	160 ± 10	780 ± 54	750 ± 160
hCNT1	22 ± 3	31 ± 1	540 ± 110
hCNT2	1200 ± 210	70 ± 6	>3000
hCNT3	35 ± 5	8 ± 1	65+4

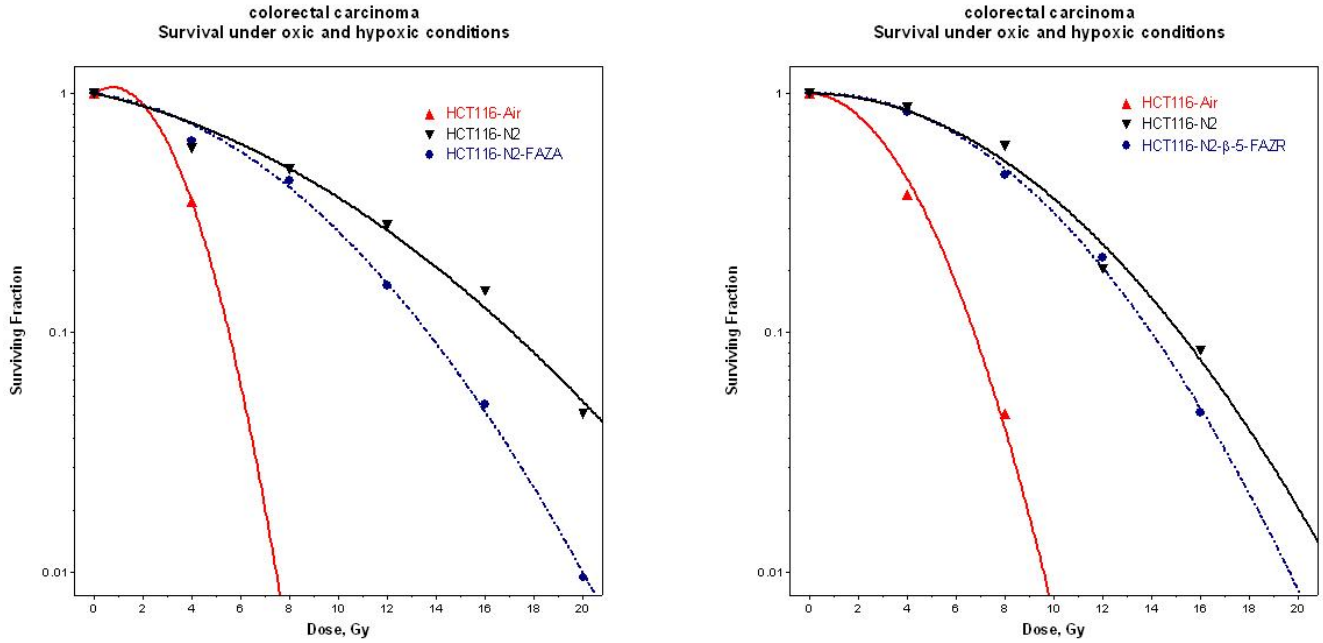

Figure 2. *In vitro* cell radiosensitization by FAZA (left) and β-5-FAZR in HCT116 colorectal carcinoma (right) cell lines. Both data sets are for 100 μM sensitizer concentrations.

The current work compared the ability of AZR, β-5-FAZR and thymidine to bind to hENT1/2 and hCNT1/2/3 by determining IC_{50} values for inhibition of [^{3}H]uridine transport into yeast producing individual recombinant hNTs. A comparison of IC_{50} values provides an indication of the rank order of apparent binding affinities of the transporters for potential permeants and/or inhibitors (23,25) and for many nucleoside analogs also predicts transportability (25). The results confirmed interaction of AZR with hENT1 and demonstrated interaction with the other hNTs, which, with the exception of hCNT2, were two to four-fold more sensitive to inhibition by thymidine than by AZR. Reduced interaction of β-5-FAZR was observed for all five hNTs, suggesting that its transportability into human cells is poor. This result was not unexpected since C-5' chlorination of uridine has been shown to diminish interaction with hENT1/2 and hCNT1/2/3 relative to that of uridine (23-25).

It is documented that hypoxia reduces adenosine transport via ENT1 and recent studies have shown that hypoxic cells also exhibit reduced levels of ENT1 mRNA (35). Other studies, which related the levels of ENT1 and ENT2 to transcriptionally dependent decreases in mRNA, have found that

ENT1 and ENT2 mRNA levels are dependent on hypoxia inducible factor 1 (HIF-1) and are repressed during hypoxia (36,37). These considerations could be important in diseases for which the environment is poor in oxygen, such as intrauterine growth or gestational diabetes.

CONCLUSION

β-5-FAZR, a positional and configurational isomer of FAZA, has been synthesized and shown to function *in vitro* as a hypoxic cell radiosensitizer. hENT1/2 and hCNT1/2/3 exhibited low "apparent affinities" and thus low potential transportability for β-5-FAZR relative to AZR and thymidine, with the exception of hCNT3 for which the IC_{50} value was approximately double that for thymidine. It is likely that β-5-FAZR is transported by hCNT3. Additional *in vivo* studies are required to demonstrate improved uptake of β-5-FAZR by hypoxic tissues.

ACKNOWLEDGEMENTS

The authors are grateful to Alberta Cancer Board and the National Cancer Institute of Canada (CEC) for financial support to this project. This work was supported in part through a Proof-of-Principle grant from the Canadian Institutes of Health Research (LIW). SE was supported by a scholarship provided by the Iranian Ministry of Health and Medical Education Tehran Iran. RP was supported by the Endowed Graduate Studentship in Oncology: Recruitment Award and a Studentship from the Alberta Heritage Foundation for Medical Research. CEC is Canada Research Chair in Oncology. Ms. Kalsoom Akhtar, an IAEA-sponsored visiting scientist from Pakistan, is thanked for assistance with interpretation of several NMR spectra. Ms. T. Tackaberry is acknowledged for assistance with studies of hNTs produced in yeast.

REFERENCES

[1] Weissleder, R., Mahmood, U. Molecular imaging. Radiology, 219: 316–333, 2001.

[2] Less, J.L., Skalak, E.M., Sevick, E.M., Jain, R.K. Microvascular architecture in a mammary carcinoma: branching pattern and vessel dimensions. Cancer Res., 51: 265-273, 1991.

[3] Brown, J.M., Giaccia, A.J. The unique physiology of solid tumors: opportunities (and problems) for cancer therapy. Cancer Res., 58:1408-1416, 1998.

[4] Intaglietta, M., Myers, R.R., Gross, J.F., Reinhold H.S. Dynamics of microvascular blood flow in implanted mouse mammary tumours. Bibl. Anat., 15 Part 1: 273-276, 1977.

[5] Chaplin, D.J., Olive, P.L., Durand, R.E. Intermittent blood flow in a murine tumour: Radiobiological effects. Cancer Res., 47: 597-601, 1987.

[6] Chaplin, D.J., Trotter, M.J., Durand, R.E., Olive, P.L., Minchinton, A.I. Evidence for intermittent radiobiological hypoxia in experimental tumour systems. Biomed. Biochim. Acta, 48: 255-259, 1989.

[7] Dewhirst, M.W., Braun, R.D., Lanzen, J.L. Temporal changes in PO2 of R3230AC tumors in Fischer-344 rats. Int. J. Radiat. Oncol. Biol. Phys. 42: 723-726, 1998.

[8] Bunn, H.F., Poyton, R.O. Oxygen sensing and molecular adaptation to hypoxia. Physiol. Rev., 76: 839-885, 1996.

[9] Dachs, G.U., Stratford, I.J. The molecular response of mammalian cells to hypoxia and the potential for exploitation in cancer therapy. Br. J. Cancer, 74: S126-S132, 1996.

[10] Gray, L.H., Conger, A.D., Ebert, M., Hornsey, S., Scott, O.C. The concentration of oxygen dissolved in tissue at the time of irradiation as a factor in radiotherapy. Br. J. Radiol., 26: 638–648, 1953.

[11] Biaglow, J.E., Varnes, M.E., Roizen-Towle, L., Clark, E.P., Epp, E.R., Astor, M.B., Hall, E. Biochemistry of reduction of nitro heterocycles. J Biochem. Pharmacol., 35: 77-90, 1986.

[12] Brown, J.M., Workman, P. Partition coefficients as a guide to the development of radiosensitizers which are less toxic than misonidazole. Radiat. Res., 82: 171-190, 1980.

[13] Kumar, P., Stypinski, D., Xia, H., McEwan, A. J. B., Machulla, H-J., Wiebe, L.I. Fluoroazomycin arabinoside (FAZA): Synthesis, ^{2}H and ^{3}H-labelling and preliminary biological evaluation of a novel 2-nitroimidazole marker of tissue hypoxia. J. Label. Comp. Radiopharmaceuticals, 42: 3-16, 1999.

[14] Reischl, G., Ehrlichmann, W., Bieg, C., Kumar P., Wiebe, L.I., Machulla, H.-J. Synthesis of F-18-FAZA, a new tracer for hypoxia. Appl. Radiat. Isot., 62: 897–901, 2005.

[15] Hicks, R., et al. Unpublished results.

[16] Beck, R., Picchio, M., Seidl, S., Haubner, R., Machulla, H-J., Kumar, P., Wiebe, L.I., Schwaiger, M., Piert, M. Intratumoral distribution and correlation of ^{18}F-FAZA, ^{125}I-Gluco-RGD and HIF-1α expression in a murine tumor hypoxia model. J. Nuc. Med. (suppl), 46:44P (abstract 126), 2005.

[17] Sorger, D., Patt, M., Kumar, P., Wiebe, L.I., Barthel, H., Seese, A., Dannenberg, C., Tannapfel, A., Osama Sabri, R.K. [^{18}F]Fluoroazomycin-arabinofuranoside ($^{18}FAZA$) and [^{18}F]Fluoro-

misonidazole (^{18}FMISO): a comparative study of their selective uptake in hypoxic cells and PET imaging in experimental rat tumors. Nucl. Med. Biol., 30: 317–326, 2003.

[18] Piert, M., Machulla, H-J., Picchio, M., Reischl, G.P., Ziegler, S., Kumar, P., Wester, J., Wiebe, L.I., Schwaiger, M. F-18 labeled Fluoroazomycin arabinoside (FAZA): Imaging tumor hypoxia with improved biokinetics. J. Nucl. Med., 46: 106–113, 2005.

[19] Solomon, B., Binns, D., Roselt, P., Wiebe, L.I., McArthur, G.A., Cullinane, C., Hicks, R.J. Modulation of intratumoral hypoxia by the epidermal growth factor receptor inhibitor gefitinib detected using small animal PET imaging. Mol. Cancer Ther., 4: 1417-1422, 2005.

[20] King, A.E., Ackley, M.A., Cass, C.E., Young, J.D., Baldwin, S.A. Nucleoside transporters: from scavengers to novel therapeutic targets. Trends Pharmacol. Sci., 27: 416-425, 2006.

[21] Ritze, L., Ng, A.M., Yao, S.Y., Graham, K., Loewen, S.K., Smith, K.M., Ritzel, R.G., Mowles, D.A., Carpenter, P., Chen, X.Z., Karpinski, E., Hyde, R.J., Baldwin, S.A., Cass, C.E., Young, J.D. Molecular identification and characterization of novel human and mouse concentrative Na+-nucleoside cotransporter proteins (hCNT3 and mCNT3) broadly selective for purine and pyrimidine nucleosides. J. Biol. Chem., 276: 2914-2927, 2001.

[22] Mirzayans, R., Andrais, B., Paterson, M.C. Synergistic effect of aphidicolin and 1-β-D-arabinofuranosylcytosine on the repair of x-ray-induced DNA damage in normal human fibroblasts. Int. J. Radiat. Biol., 6: 417-425, 1995.

[23] Zhang, J., Visser, F., Vickers, M.F., Lang, T., Robbins, M.J., Nielsen, L.P.C., Nowak, I., Baldwin, S.A., Young, J.D., Cass, C.E. Uridine binding motifs of human concentrative nucleoside transporters 1 and 3 produced in Saccharomyces cerevisiae. Mol. Pharmacol., 64: 1512–1520, 2003.

[24] Vickers, M.F., Zhang, J., Visser, F., Tackaberry, T., Robins, M.J., Nielsen, L.P., Nowak, I., Baldwin, S.A., Young, J.D., Cass, C.E. Uridine recognition motifs of human equilibrative nucleoside transporters 1 and 2 produced in Saccharomyces cerevisiae. Nucleosides Nucleotides Nucleic Acids, 23: 361-373, 2004.

[25] Zhang, J., Smith, K.M., Tackaberry, T., Visser, F., Robins, M.J., Nielsen, L.P., Nowak, I., Karpinski, E., Baldwin, S.A., Young, J.D., Cass, C.E. Uridine binding and transportability determinants of human concentrative nucleoside transporters. Mol. Pharmacol., 68: 830–839, 2005.

[26] Mannan, R.H., Somayaji, V.V., Lee, J., Mercer, J.R., Chapman, J.D., Wiebe, L.I. Radioiodinated 1-(5-Iodo-5-deoxy-β-D-arabinofuranosyl)-2-nitroimidazole (Iodoazomycin Arabinoside: IAZA), a novel marker of tissue hypoxia. J. Nucl. Med., 32: 1764-1770, 1991.

[27] Kumar, P., Wiebe, L.I., Atrazheva, E, Tandon, M. An improved synthesis of α-AZA, α-AZP and α-AZG, the precursors to clinical markers of tissue hypoxia. Tet. Lett., 42: 2077-2078, 2001.

[28] Vander Kelen, G.P., Eeckhaut Z. C13 splitting in protein and fluorine nuclear magnetic resonance spectra by halogenated aliphatic compounds. J. Mol. Spectroscopy, 10: 141-151, 1963.

[29] Sakaguchi, M., Larroquette, C.A., Agrawal, K.C. Potential radiosensitizing agents. 6. 2-Nitro-imidazole nucleosides: arabinofuranosyl and hexopyranosyl analogues. J. Med. Chem., 26: 20-24, 1983.

[30] Agrawal, K.C., Rupp, W.D., Rockwell, S. Radiosensitization, pharmacokinetics, and toxicity of a 2-nitroimidazole nucleoside (RA-263). Radiat. Res., 105: 227-239, 1986.

[31] Jette, D.C., Wiebe, L.I., Flanagan, R.J., Lee, J., Chapman, J.D. Iodoazomycin riboside (1-(5'-iodo-5'-deoxyribofuranosyl)-2-nitroimidazole), a hypoxic cell marker. Synthesis and in vitro characterization. Radiat. Res., 105: 169-179, 1986.

[32] Pedersen, J.E., Barron, G., Chapman, J.D. Azomycin riboside: a new radiosensitizer. Int. J. Radiat. Oncol. Biol. Phys., 8: 415-418, 1982.

[33] Kumar, P., Ohkura, K., Beiki, D., Wiebe, L.I., Seki, K-I. Synthesis of 1-β-D-(5-Deoxy-5-iodoarabino-furanosyl)-2-nitroimidazole (β-IAZA): A novel marker of tissue hypoxia. Chem. Pharm. Bull. 51: 399-403, 2003.

[34] Jarvis, S.M., Chapman, J.D., Ngan-Lee, J., Rutledge, K.A., Barr, P.J., Paterson, A.R. Azomycin riboside, a sugar homologue of misonidazole with favorable radiosensitizing properties. Cancer Res., 42: 4358-63, 1982.

[35] Chaudary, N., Naydenova, Z., Shuralyova, I., Coe I.R. Hypoxia regulates the adenosine transporter, mETN1, in the murine cardiomyocyte cell line, HL-1. Cardiovasc. Res., 61: 780-788, 2004.

[36] Podgorska, M., Kocbuch, K., Grden, M., Szutowicz, A., Pawelczyk, T. Reduced ability to release adenosine by diabetic rat cardiac fibroblasts due to altered expression of nucleoside transporters. J. Physiol., 576: 179-189, 2006.

[37] Eltzschig, H.K., Abdulla, P., Hoffman, E., Hamilton, K.E., Daniels, D., Schönfeld, C., Löffler, M., Reyes, G., Duszenko, M., Karhausen, J., Robinson, A., Westerman, K.A., Coe, I.R., Colgan, S.P. HIF-1-dependent repression of equilibrative nucleoside transporter (ENT) in hypoxia. J. Exp. Med., 202: 1493-1505, 2005.